



UNIVERSITAT POLITÈCNICA  
DE CATALUNYA  
BARCELONATECH

# UPCommons

**Portal del coneixement obert de la UPC**

<http://upcommons.upc.edu/e-prints>

---

© 2018. Aquesta versió està disponible sota la llicència CC-BY-NC-ND 4.0 <http://creativecommons.org/licenses/by-nc-nd/4.0/>

© 2018. This version is made available under the CC-BY-NC-ND 4.0 license <http://creativecommons.org/licenses/by-nc-nd/4.0/>

---

# On Osmotic Heat Engines Driven by Thermal Precipitation-Dissolution of Saturated Aqueous Solutions

Francisco J. Arias\*

*Department of Fluid Mechanics, University of Catalonia,  
ESEIAAT C/ Colom 11, 08222 Barcelona, Spain*

Cyclic thermal precipitation and dissolution of saturated aqueous solutions and its significance with regard to osmotic heat engines (OHEs) is discussed. Here, the thermal dependence of the solubility of aqueous solutions is harnessed by alternating thermal solute precipitation and dissolution when heat is either applied (by heating the solution) or extracted (by cooling the solution) depending of the given solution. Utilizing a simplified physical model, it is shown that by the proper choice of the concentration of the given aqueous solution it is possible a closed cycle. Because in contrast with traditional OHEs working with dilute solutions, here the proposed engine operates at saturation concentrations and therefore the approximation of dilute solution might not be valid, an osmotic coefficient was included in the calculations to take account the deviation from the ideal case of a dilute solution. The expression for the extractable energy per unit of volume of solution as well as the thermal efficiency of the heat engine were derived considering the spontaneous change in the Gibbs free energy and enthalpy of precipitation for the thermal efficiency of the engine. The specific case for  $\text{Na}_2\text{SO}_4$  was analyzed and it was found a percentage of Carnot efficiency as high as 23 % which is a little larger than the efficiencies reported by traditional OHEs. Even if its is considered several irreversibilities and uncertainties an assumed an efficiency equal than traditional OHEs, the proposed heat engine eliminates the need of evaporation to re-concentrate the draw solution and then the constraint of working with solutions with high vapor pressures where here a solution can be placed as close as the saturation point by controlling its initial concentration.

**Keywords.** *Thermal solubility of aqueous solutions; Osmotic heat engines; Pressure-retarded osmosis, (PRO); Salinity power*

## I. INTRODUCTION

The possibility to extract energy from salinity gradients has been investigated from the second half of the last century [1]-[11]. In the las decades, however, and due to the growing interest for the use of clean renewable energy sources, the salinity gradient power or also called as *blue energy* has shown a revival of interest on the possibilities of harnessing the energy released during the spontaneous mixing of two solutions of different salinities [12]-[33].

Although several process has been investigated for efficient conversion of the salinity gradient into useful work based on flow through semipermeable membranes, (e.g., reverse electrodialysis, capacitive mixing, ion-selective membranes), nevertheless pressure retarded osmosis (PRO) is the technique most widely studied. In this technique, a semipermeable membrane allows the solvent to pass to the concentrated solution side by osmosis generating a hydraulic pressure which can be used to generate power by, say driven the flow through a turbine.

In connection with thermal process, one application of

the PRO process is in osmotic heat engines (OHEs) or also called as closed cycle-PRO processes. OHEs have been proposed by several investigators intended to use low temperature heat to recycle an osmotic agent, see for example the early works by [2]-[5], and most recently, by [34]. Those heat engines operates with a poor efficiency limited by the high heat of vaporization of the working fluid (vaporization is needed to re-concentrate the draw solution (high salinity solution) by vaporizing a portion of the water into steam, [34]).

The object of this work was to analyze a different approach based in the thermal properties of aqueous solutions in which when a saturation temperature is attained solute can precipitate or dissolve into the solvent. Here, it will be demonstrated that by the proper choice of the concentration of a given aqueous solution an osmotic heat engine can be driven by the thermal dependence of the solubility of the solution -coefficient of thermal solubility, by alternating solute and solvent precipitation and mixing when heat is either applied (by heating the solution) or extracted (by cooling the solution) depending of the specific thermal dependence of the solubility of given solution.

This kind of OHE besides the transformation of heat into mechanical work, has a number of important applications, for example, as a mass and heat transport

---

\*Corresponding author: Tel.: +32 14 33 21 94; Electronic address: francisco.javier.arias@upc.edu

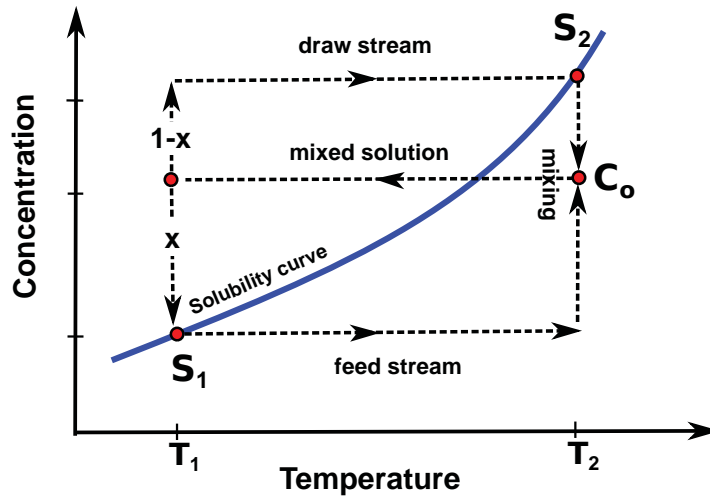


FIG. 1: The basis of the proposed osmotic heat engine driven by the precipitation of saturated aqueous solutions.

mechanism in what might be called *thermo-osmotic convection* similar to that of natural convection but with one important difference. Whereas in natural convection the fluid motion is generated by density differences in the fluid occurring due to temperature gradients and always under the action of a gravitational field, [38],[39], in *thermo-osmotic convection* the convective motion is driven by the thermal differences of solubility and any gravitational field is needed. Alternative mechanisms to natural convection have been investigated in the past. For example, the convection driven by Marangoni effect (also called the Gibbs-Marangoni effect) where mass transfer is promoted along an interface between two fluids due to surface tension gradient. In the case of temperature dependence, this phenomenon is generally referred as Bénard-Marangoni convection or thermo-capillary convection, [40]. However, Marangoni convection is restricted to the presence of an interface and if compared with natural convection in most practical applications can be disregarded, [41]. Another type of non-gravitational thermal convection is the thermophoresis (also thermomigration, thermodiffusion, the Soret effect, or the Ludwig-Soret effect) in which mixtures of mobile particles display different responses to the force of a temperature gradient, nevertheless the phenomenon is observed at the scale of one millimeter or less. In regard to the use of solutions, there are not any work exploring the potential use of them for driven a convective mechanism per se, and so far only solutal thermodiffusion aspects have been addressed, as far as the author knows, see for example, [45]-[47]. Most recently, the possibility to run a solar thermosyphon by working with a solution was investigated, [42],[43]. In those works, convection was induced either by buoyancy-induced force owing to dependence of density with salt concentration or by evaporation at collectors.

Finally, one of the attractiveness of the proposed

concept is the availability of a wide range of salts and with a wide range of saturation temperatures.

## II. METHODS

In this section a first theoretical assessment of the concept will be derived. The model as well as the maximum extractable energy reported result from unavoidable idealizations which are always required if general analytical expression are desired. Nevertheless with such idealizations an upper limit can be obtained and therefore encouraging or not further research as well as providing an important guidance in future efforts to analyze the problem.

### A. Statement of the core idea

To begin with, let us consider the thermal cycle depicted in Fig. 1 in which, for the sake of generality, an aqueous solution which increase its solubility with temperature was chosen, however, the argument can be used for solutions with contrary behavior ( see for example the case for  $\text{Ce}_2(\text{SO}_4)_3$  shown in Fig. 3). Let us fix the given solution with an initial temperature, say  $T_2$  and concentration  $C_0$  below its saturation concentration  $S_2$  at that temperature, i.e, the solution is "under saturated". Now, if this solution is cooled from the initial temperature  $T_2$  to  $T_1$  and if the initial concentration  $C_0$  is now higher than the saturation solubility  $S_1$  at  $T_1$ , then the initial unsaturated solution is now "super saturated" and precipitation takes place.

Therefore, so far the only imposed requirement in our argument is that the initial concentration of the aqueous solution **should be under saturated at its initial tem-**

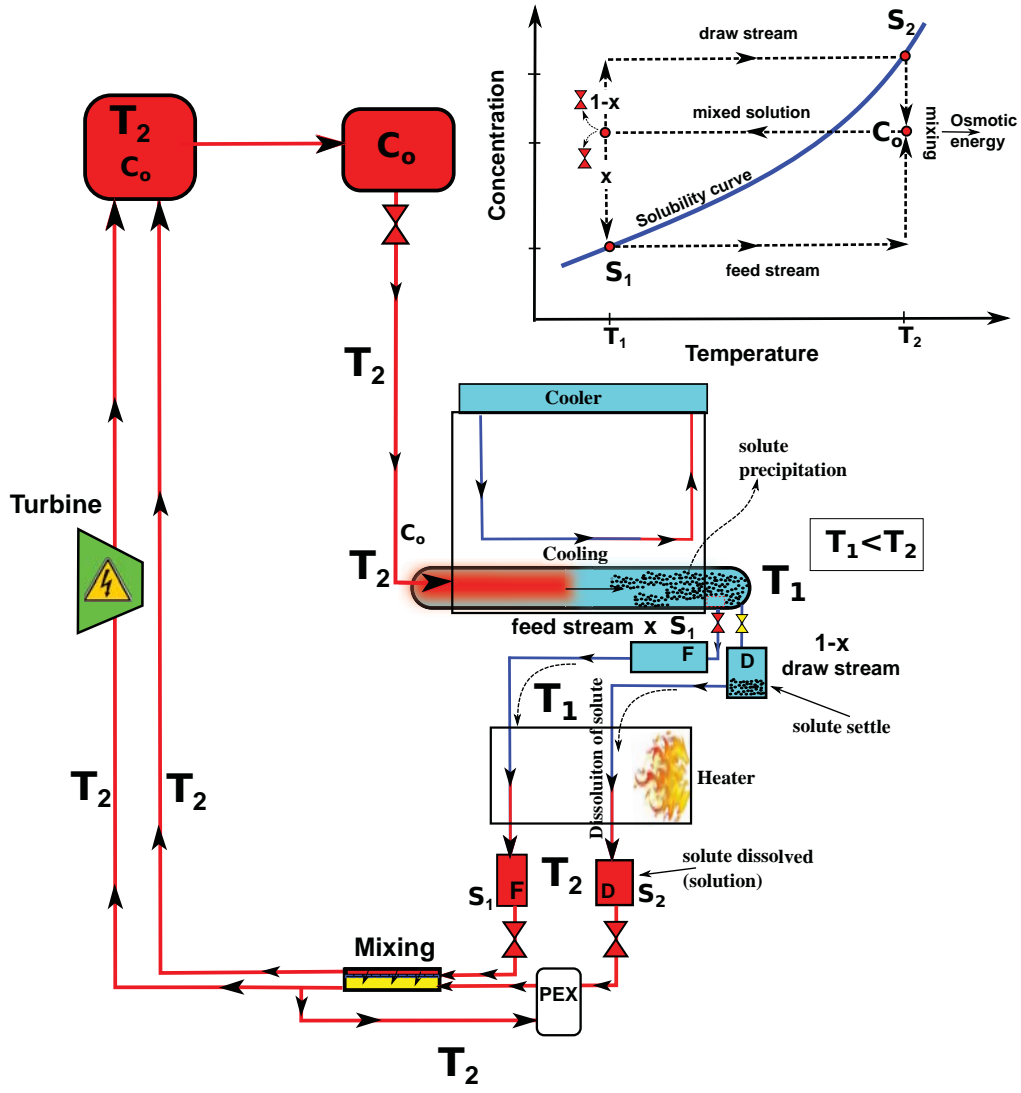


FIG. 2: Sketch for a possible osmotic heat engine running by the cyclic thermal precipitation/mixing of an aqueous solution.

perature and super saturated at the final temperature satisfying

$$S_2 > C_o > S_1 \quad (1)$$

Once supersaturation take place, the excess of particles of solute precipitate and can be separated by using a proper filter. At this moment we have two separate solutions, on one hand a solution depleted in solute which is known as *supernate* with a concentration  $S_1$  equal to its saturation at temperature  $T_1$  and on the other hand a solution where the precipitated solute is settle. Referring to Fig. 1, let us now separate the supersaturated solution into a volume fraction of the depleted solution, say,  $(x)$  and the rest of volume, i.e., a fraction  $(1 - x)$  containing the precipitated. After this separation, both solutions are heated again and recovering their initial temperature  $T_2$  and as a result, their solubility again increase. This makes that the settle

solute in the fraction  $(1 - x)$  is totally dissolved. We have at this point two separated homogenous solutions with two different concentrations and with the initially precipitated solute perfectly dissolved in one of them. Now, if the proper fraction  $x$  was chosen, then it is possible that the dissolved fraction  $(1 - x)$  get the maximum solubility at  $T_2$ , i.e.,  $S_2$ . In summary, from an initial solution with concentration  $C_o$  at  $T_2$ , and after a change in temperature to  $T_1$  we are forming a low-salinity solution  $S_1$  and a high-salinity solution  $S_2$ . Now, if both solutions are brought together by using a semipermeable membrane, it is possible harnessing the osmotic energy released.

Fig. 2 shows is a sketch what a osmotic heat engine working with the before mentioned principle would look. Referring to this figure, an initial solution with concentration  $C_o$  and temperature  $T_2$  enters a precipitator-module where the solution is cooled to a temperature  $T_1$  by putting in contact with a cold reservoir, and then

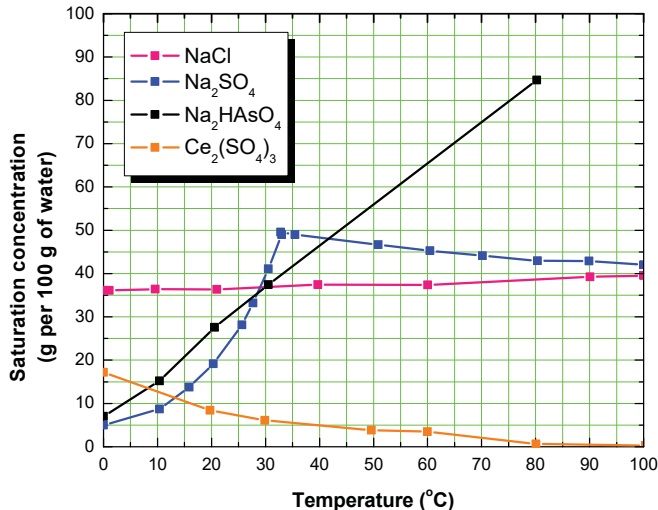


FIG. 3: Solubility vs. temperature for a variety of salts. Data are taken from [44].

becomes supersaturated. The solution, after passing through the precipitator, is separated into two solutions: one with a volume fraction  $(1 - x)$  where is the precipitated solute, and other with a volume fraction  $x$  where is the solution depleted in solute. Although the process of separation of the particles of solute is specific for a given particular design, however it could be entirely driven by the self motion of the fluid owing to the very small size of particles with Stokes number  $Stk \ll 1$  and then following the fluid streamlines closely. Therefore by interposing a, say, microporous-filter, the solute can be separated by simple bifurcation of its path from the main solvent. Finally, after passing through a heat exchanger where it is heated by a heat source (e.g., the Sun), the two solutions recover the initial temperature  $T_2$  in their respective separated containers. At this point, the fraction of volume  $(1 - x)$  which contain the precipitated solute redissolves (because at  $T_2$  the solubility increase) and form a dissolved solution with concentration  $S_2$ .

Now, the draw solution (fraction  $(1 - x)$ ) with solubility  $S_2$  and the feed solution (fraction  $x$ ) with solubility  $S_1$  enter the membrane module. In this membrane-module, driven by the osmotic pressure differences across the membrane, water molecules permeate from the feed stream to the draw stream, increasing the flow rate and diluting the pressurized draw stream while decreasing the flow rate and concentrating the feed stream. Then, the diluted draw stream and the concentrate feed stream exit the membrane-module and are mixed. The exiting pressurized draw-feed mixture flows through a pressure exchanger (PEX), which transfer pressure to the incoming mix solution to propel this through the precipitator and then running the closed cycle.

Bearing this simplified scheme in mind, we can proceed with some theoretical treatment.

First of all, we need to calculate the required volume fraction  $x$  which allows the mentioned cycle. This calculation may be easily found by a balance of mass of the solute before and after the precipitation take place as

$$C_o = S_1 x + S_2(1 - x) \quad (2)$$

and then the volume fraction of the feed given by

$$x = \frac{S_2 - C_o}{S_2 - S_1} \quad (3)$$

where the mixed solution  $C_o$  must satisfy the relationship Eq.(1), i.e.,  $S_2 > C_o > S_1$ .

Therefore by knowing the initial concentration of a given solution  $C_o$  at a given temperature, we can now the saturation concentration at that temperature  $S_1$  and with the temperature difference  $\Delta T$  between the hot and cold reservoirs we can find  $S_2$  and then the optimized volume fraction  $x$ . Now, the next step is the calculation of the extractable energy from this engine.

## B. Extractable energy

It is known that the maximum energy available from the osmotic mixing of an dilute solution is equal to the Gibbs free energy of mixing  $\Delta G$ . The change in Gibbs energy per volume for a dilute solution is given by [51] an others

$$\Delta G = iRT [c_M \ln(c_M) - x c_F \ln(c_F) - (1 - x) c_D \ln(c_D)] \quad (4)$$

where  $i$  is the vant'Hoff factor for electrolytes (e.g,  $i = 3$  for  $\text{Na}_2\text{SO}_4$ ;  $i = 2$  for  $\text{NaCl}$ , etc...),  $R$  is the gas constant.  $c_M$ ,  $c_F$ ;  $c_D$  are the concentrations of the mixture, feed and draw, respectively.

For our case  $C_o = c_M$ ;  $S_1 = c_F$  and  $S_2 = c_D$  and then

$$\Delta G = iRT [C_o \ln(C_o) - x S_1 \ln(S_1) - (1 - x) S_2 \ln(S_2)] \quad (5)$$

The ideal approximation given by Eq.(4) which has been so far used in traditional OHEs, (see for example [2]-[5], and most recently, by [34]) is only valid for dilute solutions i.e., with low solute concentrations. However, in working at saturation level this assumption might not be true. Indeed, although the saturation solubility of salts can be very low (see for example the solubility of barite  $\text{BaSO}_4$  with concentrations of solubility less than 4 ppm at a constant temperature of  $100^\circ\text{C}$  and atmospheric pressure,[52],[53]) and then the ideal approximation is valid, nevertheless for the general case saturation



$$\Delta n_m = C_o - S_1 \quad (13)$$

which considering Eq.(3) becomes

$$\Delta n_m = (1 - x)(S_2 - S_1) \quad (14)$$

and then

$$Q_{in} = \bar{c}_p \Delta T \bar{\rho} + h_d(1 - x)(S_2 - S_1) \quad (15)$$

#### • Discussion

To obtain some idea of the extractable energy predicted by Eq.(7) as well as the thermodynamic efficiency of the proposed engine, we will analyze the specific case for the aqueous solution  $\text{Na}_2\text{SO}_4$  with the following parameters:

$\Delta T = 30 \text{ K}$ ; with  $T = 273 \text{ K}$ , The heat of precipitation or crystallization is  $h_p = 1.18 \text{ kJ/mol}$  taken from [56]; the heat capacity and density are shown in Fig. 5 from [57], and then an average capacity  $\bar{c}_p = 3300 \text{ J/(kg-K)}$  is assumed considering a saturation close to 3 molality (see Fig.3), and the density as  $\bar{\rho} = 1300 \text{ kg/m}^3$ . A vant'Hoff factor  $i = 3$  for  $\text{Na}_2\text{SO}_4$ , and the osmotic coefficient  $\theta = 0.67$  from Fig. 6. The resulting curves are shown in Fig. 7 and Fig. 8 for the extractable energy and the heat input  $Q_{in}$ , respectively. In Fig. 8, the percentage of Carnot engine efficiency is shown where the Carnot efficiency is calculated as

$$\eta_C = \frac{\Delta T}{T + \Delta T} \quad (16)$$

Referring to Fig. 9, it is seen that the percentage of Carnot efficiency can be as large as 23% or thereabouts. By comparison, the reported value for a traditional OHEs driven by evaporation as discussed by [34] is on 16% of Carnot efficiency, therefore if one consider several irreversibilities inherent in the cycle, fluid friction, heat loss to the surrounding not considered in our calculations, then we can say that the percentage of Carnot efficiency can be similar than the traditional OHEs.

#### D. solubility vs evaporation

We have see, that at least for the specific case of  $\text{Na}_2\text{SO}_4$  de Carnot efficiencies can be in the same order than traditional OHEs driven by evaporation.

It is interesting to analyze the advantages in doing separation by thermal precipitation rather than by evaporation, to do this we pprceed as follows:

Let us consider the Raoult's law which allow us to calculate the variation of the vapor pressure of a ideal solution when concentration of the solute changes as

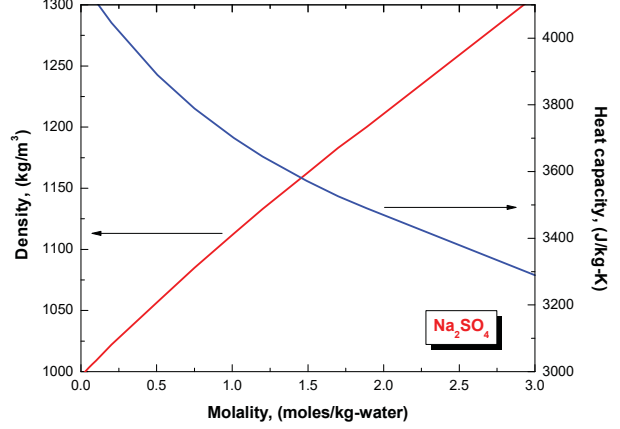


FIG. 5: Experimental heat capacity and density for  $\text{Na}_2\text{SO}_4$  solution at  $25^\circ\text{C}$ , [57].

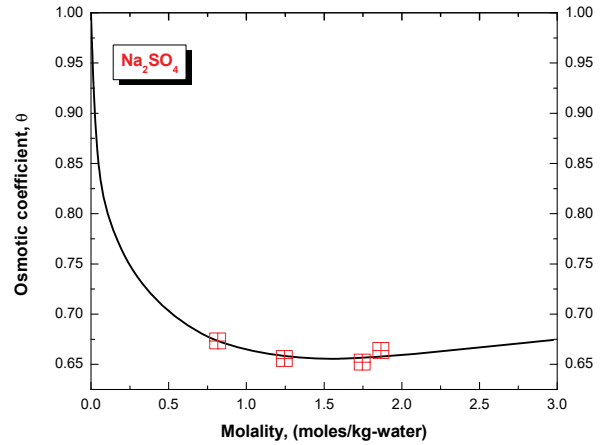


FIG. 6: Osmotic coefficient for  $\text{Na}_2\text{SO}_4$  at  $50^\circ\text{C}$ . solid line calculated using an Universal Quasi-Chemical Activity Coefficients (UNIQUAC) model, and symbol by experimental data from [58]

$$p_{sl} = \chi_w p_{wo} \quad (17)$$

where  $p_{sl}$  is the observed vapor pressure of the solution,  $p_{wo}$  is the vapor pressure of the pure solvent (e.g., water), and  $\chi_w$  is the mole fraction of solvent, i.e.,  $\chi_w = \frac{n_w}{n_w + n_s}$  where  $n_w$  is the number of moles of solvent and  $n_s$  the number of moles of solute. Eq.(17) may be rewritten as function of the molality of the solution  $m_s$  as



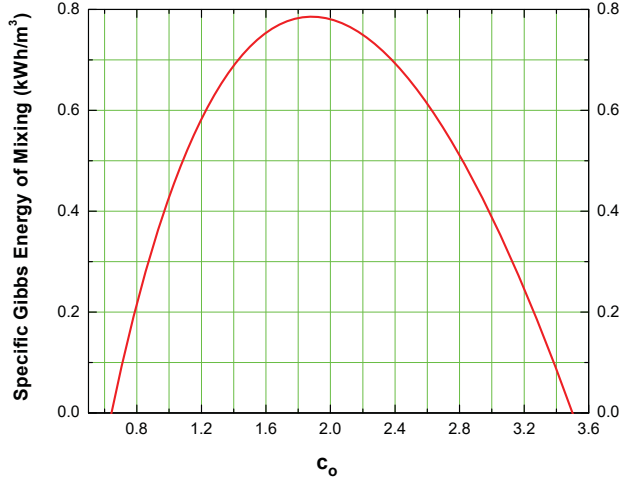


FIG. 7: Specific Gibbs free energy of mixing for  $\text{Na}_2\text{SO}_4$  solution with  $\Delta T = 30$  K;  $T = 273$  K;  $S_1$  and  $S_2$  from Fig. 3 and the fraction of volume  $x$  calculated from Eq.(3).

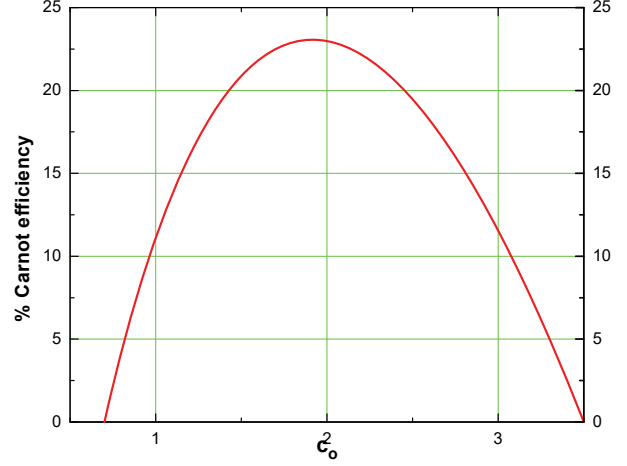


FIG. 9: The engine efficiency as a percentage of Carnot engine efficiency.

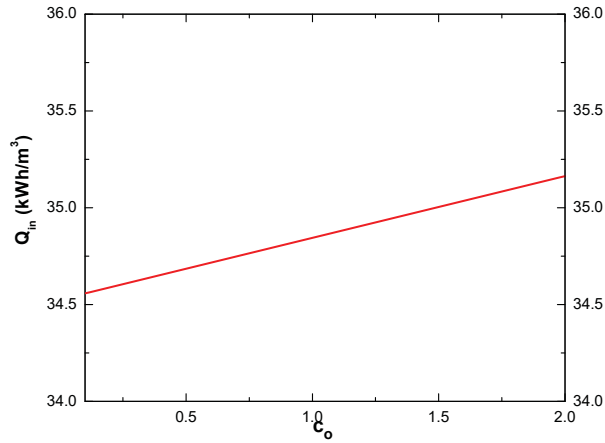


FIG. 8: Heat input calculated from Eq.(15).

$$\frac{p_{sl}}{p_{wo}} = \frac{1}{1 + m_s M_w} \quad (18)$$

where  $M_w$  is the molar mass of the solvent.

In Eq.(18), we can see that the vapor pressure of the solution is only affected by the concentration when the molality is very high and even higher than the allowable solubility. Indeed, by looking at Fig. 3, it is easy to see that molalities of saturation could be close to  $m_s = 5$  mol/kg-water at best, and then  $M_s M_w \ll 1$  or  $p_{sl} \approx p_{wo}$ , i.e., the changes of the vapor pressure of the solution can be neglected.

$$p_{sl} \approx p_{wo} \quad (19)$$

Therefore, if we want an OHE driven by evaporation, it is mandatory to choose a working fluid with a vapor pressure very close to the atmospheric pressure (or the pressure of the system) to allow evaporation. If the vapor pressure is very low at the environment temperature, then there will be necessary a large expenditure of heat to increase the vapor pressure allowing evaporation. However, with the discussed method, the separation of the solute is not by evaporation but by thermal precipitation, and then there is a large freedom degree to choose a given aqueous solution and then fixing as close as is desired the solubility (precipitation) just by increasing or reducing the concentration without need to expenditure of heat (see Fig. 3).

The above reflection is depicted in fig. 10. In this it is desired that a given solution be closer to the solubility curve (top) or the vapor pressure (bottom). For our method (top) it is only necessary increase the concentration of the salt, but for a classical OHS, because the vapor pressure changes very little with concentration, it is necessary to increase the temperature of the working fluid which can be a large expenditure of heat, and then making mandatory the selection of high vapor pressures at the environment temperature which reduces substantially the availability of materials.

### E. Growth of solute particles

In preceding section it was assumed that once supersaturation occurs at the precipitator module, the solute may be continuously separated from the main solvent



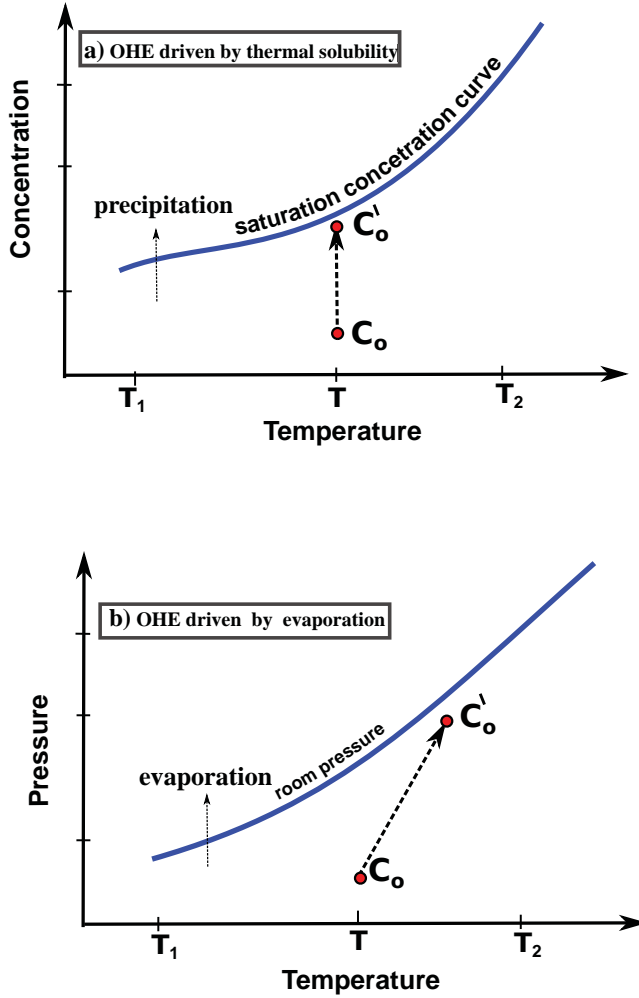


FIG. 10: In this figure given an aqueous solution it is desired a solute separation with the minimum expenditure of heat. (a)-top: in the proposed method, this can be easily conducted by increasing the concentration of the given solution. (b)-bottom: with traditional evaporative method because the negligible dependence of the vapor pressure with the concentration it is required heating the solution, as a result an initial volatile solution is necessary and then limiting the available solutions.

by using a microporous filter. However, to do this, it is necessary a certain time for allowing the growth of the solute particles from the ultramicroscopic size in the nucleation stage to the desired microscopic size. The determination of this time is important for thermo-osmotic convection design because, as we will see, set a limit in the minimum dimensions of the precipitator.

Two begin with, immediately after nucleation, the solute particles will start to grow, first governed by diffusion and after attaining a certain size by fluid motion,[60].

Therefore, the total time required for separation  $t_t$ , may be rewritten as

$$t_t = t_d + t_f \quad (20)$$

where  $t_d$  and  $t_f$  are the time for growth of particles governed by diffusion and fluid motion, respectively.

The time limited by diffusion is given by Smoluchowski,[59],

$$t_d = \frac{\frac{N_o}{N_d} - 1}{K_A N_o} \quad (21)$$

where  $N_d$  is the number of mono-sized particles per volume attained during the diffusion -limited growth, which typically is around  $1 \mu\text{m}$  particles in diameter,[60],  $N_o$  is taken as the initial number concentration of dissolved solute molecules, and the constant  $K_A$  is determined by the diffusivity and the diameter of the molecules that are adding to the particles.

Considering spherical particles, this constant can be approximated as, [60]

$$K_A = \frac{8\kappa T}{\mu} \quad (22)$$

where  $\kappa$  is the Boltzmann constant,  $T$  is the absolute temperature, and  $\mu$  is the liquid viscosity. Therefore Eq.(21) may be rewritten as, [60]

$$t_d = \frac{3\mu}{8\kappa T} \frac{\frac{N_o}{N_d} - 1}{N_o} \quad (23)$$

On the other hand, the time limited by fluid motion is given by

$$t_f = \frac{\pi \ln \frac{N_d}{N_f}}{4\alpha\varphi_f\gamma} \quad (24)$$

where  $N_f$  is the final particle number concentration,  $\alpha$  is the collision effectiveness factor (fraction of collisions that result in permanent aggregates),  $\varphi_f$  the final volume fraction of the particles, and  $\gamma$  is the shear rate (velocity gradient). Therefore, inserting Eq.(24) and Eq.(23) into Eq.(20) one obtains

$$t_t = \frac{3\mu}{8\kappa T} \frac{\frac{N_o}{N_d} - 1}{N_o} + \frac{\pi \ln \frac{N_d}{N_f}}{4\alpha\varphi_f\gamma} \quad (25)$$

Finally, if the flow rate of solution is  $Q$ , then the precipitator module should be at least with a volume given by

$$V_{pr} \geq Qt_t \quad (26)$$

to allow the formation of micro particles of solute and then their separation. On the other hand the flow rate of the fluid is related with the heat extraction power as

$$Q = \frac{W_t}{c_p \rho \Delta T} \quad (27)$$

where  $W_t$  is the thermal power,  $c_p$  the specific heat,  $\rho$  the density, and  $\Delta T$  the increase of temperature. Thus, the volume of the precipitator is given by

$$V_{pr} \geq \frac{W_t t_t}{c_p \rho \Delta T} \quad (28)$$

### • Discussion

To obtain some idea of the total time  $t_t$  predicted by Eq.(25) and the the volume of the precipitator-module, we assume some values of the parameters for  $\text{Na}_2\text{SO}_4$ . From Fig. 3: an initial concentration  $c_i = 0.5 \text{ g/cm}^3$ , a molecular weight for  $\text{Na}_2\text{SO}_4$  of  $142.04 \text{ g/mol}$ , and then an initial concentration of  $N_o = 2.12 \times 10^{21} \text{ molecules/cm}^3$ .

The growth governed by diffusion occurs until particles attain a limiting particle size between  $0.1 \mu$  to  $1 \mu\text{m}$ , [60], thus, the concentration  $N_d$  when growth by fluid motion starts is calculated as  $N_d = \frac{c_i}{\rho_p V_d}$ , where  $\rho_p$  is the density of the particle of solute, and  $V_d$  is its volume. By assuming that the growth by fluid-motion starts with a radius of particle of  $0.1 \mu\text{m}$ , and then  $V_p = \frac{4\pi r_p^3}{3} = 4.18 \times 10^{-15} \text{ cm}^3$ , with a density for  $\text{Na}_2\text{SO}_4$  of  $\rho_p = 2.66 \text{ g/cm}^3$ , we obtain  $N_d = 4.49 \times 10^{13} \text{ particles/cm}^3$ . If wish desire a final size of particles with a radius  $1 \mu\text{m}$ , then proceeding as before,  $N_f = \frac{c_i}{\rho_p V_f}$  with  $V_f$  the final volume of the particle of solute, which with  $r_f = 1.0 \mu\text{m}$  we get,  $N_f = 4.48 \times 10^{10} \text{ particles per cm}^3$  wit a volume fraction of the particles  $\varphi_f = V_p N_f$ , or  $\varphi_f = 0.18$ . Finally, the collision effectiveness factor  $\alpha$  is measured experimentally by the fraction of collisions leading to permanent aggregation, and although the calculation of  $\alpha$  based on the DLVO theory calculation is possible, nevertheless, large discrepancies are usually observed between the experimental and the theoretical predictions. nevertheless, this factor could be between 0.01 to 0.1, so, for preliminary assessment let us consider  $\alpha = 0.05$ . Finally the shear rate for a pipe of radius  $R$  and a volumetric flow rate  $Q$  can be assumed as (see appendix),

$$\gamma = \frac{4Q}{\pi R^3} \quad (29)$$

or by considering Eq.(27) as function of the power to be extracted

$$\gamma = \frac{4W_t}{c_p \rho \pi R^3 \Delta T} \quad (30)$$

For the sake of illustration, if in our case we want to extract, say,  $400 \text{ W}$  by using typical pipes of radius  $R = 0.5 \text{ cm}$ , and with  $\Delta T = 30 \text{ K}$  and a heat capacity similar than pure water  $c_p = 4180 \text{ J/(kg K)}$ , we obtain  $\gamma = 32.44 \text{ s}^{-1}$ .

With a dynamic viscosity  $\mu = 10^{-3} \text{ kg/(m s)}$  and the calculated values we obtain from Eq.(25) a total time for the micrometric growing of the solute particles of  $t_t = 37 \text{ s}$ , which by taking Eq.(28) with our power as  $400 \text{ W}$ , we will need a dedicated volume for the precipitator module around  $0.1 \text{ liters}$ .

### III. SUMMARY OF RESULTS AND CONCLUSIONS

An osmotic heat engine working by the cyclic thermal precipitation and mixing of aqueous solutions close to the saturation temperature was discussed and the theoretical basis of such a heat engine outlined. Some interesting conclusions result from this preliminary work as follows:

- (a) Thermal dependence of solubility of aqueous solution can be used to run a heat engine with closed cycle by the proper choice of the concentration of the aqueous solution.
- (b) A sort of thermo-osmotic convection can be promoted no requiring any gravitational field.
- (c) The percentage of Carnot efficiency can be equal or larger than traditional OHEs working by evaporation to re-concentrate the draw solution.
- (d) A given aqueous solution can be as close as the solubility saturation at a given temperature by fixing its initial concentration and then reducing the expenditure of heat. In contrast, traditional OHEs, working by re-concentrating the draw by evaporation, they need to use solutions with a high vapor pressure or otherwise a large expenditure of heat will be necessary. This is because the effect of concentration on the vapor pressure of the solution is very small.

In addition, this kind of heat osmotic engine rises some new questions. One of them is on the operational recyclability of an aqueous solution experiencing cyclic thermal precipitation and mixing. So far, such a closed cycles of precipitation/mixing have not been studied because no practical application have been found, as far as the author knows. The possible problem of recyclability could feature a similar problem as found in other technologies as for example in phase change materials for thermal storage and the interaction/corrosion with vessels and containers. Unfortunately, and as aforementioned, no available data was found in the literature on the recyclability of precipitation/mixing on aqueous solutions.

#### IV. APPENDIX

##### Shear rate

If we assume a low Reynolds number -which is consistent with the kind of convective motion expected, then the shear rate for a pipe in terms of the volumetric flow rate  $Q$  and the inner pipe radius  $R$  is given by,[62]

$$\gamma = \frac{4Q}{\pi R^3} \quad (31)$$

However, the some part of the energy released from the osmosis process can be used to stir the solution with a motor. In this case, the average shear rate can be estimated by the following equation developed by Camp and Stein, [63].

$$\bar{\gamma} = \left( \frac{W_s/V}{\rho\eta} \right)^{\frac{1}{2}} \quad (32)$$

where  $W_s$  is the power of the stirrer,  $V$  the volume of the vessel, and  $\rho$  and  $\nu$  are the density and kinematic viscosity of the liquid.

##### NOMENCLATURE

$a$  = activity  
 $c$  = concentration  
 $\bar{c}_p$  = equivalent heat capacity of the solution  
 $D$  = diameter of the pipe  
 $g$  = gravity  
 $\Delta G$  = free Gibbs energy per unit volume of solution  
 $h_d$  = enthalpy of dissolution  
 $h_p$  = enthalpy of precipitation,  $h_p = -h_d$   
 $h_s$  = sensible heat  
 $i$  = the vant 'Hoff factor for electrolytes  
 $K_A$  = parameter defined by Eq.(22)  
 $l$  = length of the pipe  
 $m_s$  = molality  
 $\bar{m}$  = molecular weight of the solution  
 $M_s$  = molar mass of the solute  
 $M_w$  = molar mass of the solvent  
 $n_s$  = moles of solute  
 $n_w$  = moles of solvent  
 $\Delta n_m$  = number of moles precipitated per volume  
 $N$  = number particles per volume  
 $N_o$  = initial number concentration of solute molecules  
 $p_{sl}$  = vapor pressure of the solution  
 $p_{wo}$  = vapor pressure of the pure solvent  
 $Q$  = Heat  
 $r_p$  = radius of the particle

$R$  = ideal gas constant  
 $S$  = saturated concentration  
 $\Delta T$  = difference temperature  
 $T$  = temperature  
 $t$  = time  
 $V$  = volume  
 $V_p$  = volume of the particle  
 $x$  = volume fraction of the low-concentration solution (feed)  
 $W$  = work, power

##### Greek symbols

$\alpha$  = collision effectiveness factor  
 $\rho$  = density of the solvent  
 $\rho_p$  = density of the solute  
 $\bar{\rho}$  = equivalent density of the solution  
 $\varphi_f$  = final volume fraction of the particles  
 $\gamma$  = shear rate  
 $\kappa$  = Boltzmann constat  
 $\mu$  = dynamic viscosity of the fluid  
 $\eta_{therm}$  = thermodynamic efficiency  
 $\eta_C$  = Carnot efficiency  
 $\theta$  = osmotic coefficient  
 $\chi_w$  = mole fraction of the solvent

##### subscripts symbols

$o$  = initial, reference  
 $1$  = low salinity concentration  
 $2$  = high salinity concentration  
 $D$  = high salinity concentration  
 $F$  = low salinity concentration  
 $M$  = mixture  
 $d$  = diffusion-governed growth  
 $f$  = fluid motion -governed growth  
 $t$  = total  
 $p$  = solute particle  
 $pr$  = precipitator-module

##### ACKNOWLEDGEMENTS

The author is indebted to anonymous reviewers for their suggestions and comments which led to important corrections in the final document. This research was supported by the Spanish Ministry of Economy and Competitiveness under fellowship grant Ramon y Cajal: RYC-2013-13459.

##### V. REFERENCES

- 
- [1] Pattle RE. Production of electric power by mixing fresh and salt water in the hydroelectric pile. Nature 1954;

174:(4431). <http://dx.doi.org/10.1038/174660a0>

- [2] Weingarten MH. Power generating means, US Patent 3,587,227, US (1971).
- [3] Norman RS. Water salination: a source of energy. *Science* 1974; 186: 350-352, <http://10.1126/science.186.4161.350>
- [4] Loeb S, Norman RS. Osmotic power plants. *Science* 1975; 189: 654-655, <http://10.1126/science.189.4203.654>
- [5] Loeb S. Method and apparatus for generating power utilizing pressureretarded- osmosis, US Patent 3,906,250, Ben-Gurion University of the Negev Research and Development Authority, Beersheba, Israel, US (1975).
- [6] Loeb S. Production of energy from concentrated brines by pressure-retarded osmosis?: I. Preliminary technical and economic correlations. *J. Membr. Sci* 1976; 1: 49-63, [http://10.1016/S0376-7388\(00\)82257-7](http://10.1016/S0376-7388(00)82257-7)
- [7] Jellinek HHG. Osmosis process for producing energy, US Patent 3,978,344, US (1976).
- [8] Loeb S. Method and apparatus for generating power utilizing pressureretarded- osmosis, US Patent 4,193,267, Ben-Gurion University of the Negev Research and Development Authority, Beersheba, Israel, US (1980).
- [9] Jellinek HHG, Masuda H. Osmo-power. Theory and performance of an osmo-power pilot plant. *Ocean. Eng* 1981; 8: 103-128, [http://10.1016/0029-8018\(81\)90022-6](http://10.1016/0029-8018(81)90022-6)
- [10] Lee KL, Baker RW, Lonsdale HK. Membranes for power generation by pressure-retarded osmosis. *J. Membr. Sci* 1981; 8: 141-171, [http://10.1016/S0376-7388\(00\)82088-8](http://10.1016/S0376-7388(00)82088-8)
- [11] Zentner GM, Rork GS, Himmelstein KJ. The controlled porosity osmotic pump. *Journal of Controlled Release* 1985; 1: 269-282 [http://10.1016/0168-3659\(85\)90003-3](http://10.1016/0168-3659(85)90003-3)
- [12] Loeb S. Energy production at the Dead Sea by pressure-retarded osmosis: challenge or chimera?. *Desalination* 1998; 120: 247-262, [http://10.1016/S0011-9164\(98\)00222-7](http://10.1016/S0011-9164(98)00222-7)
- [13] Post JW, Veerman J, Hamelers HVM, Euverink GJW, Metz SJ, Nymeijs K, et al. Salinity-gradient power: evaluation of pressure-retarded osmosis and reverse electrodialysis. *J. Membr. Sci* 2007; 288: 218-230, <http://10.1016/j.memsci.2006.11.018>
- [14] Skilhagen SE, Dugstad JE, Aaberg RJ. Osmotic power - power production based on the osmotic pressure difference between waters with varying salt gradients. *Desalination* 2008; 220: 476-482, <http://10.1016/j.desal.2007.02.045>
- [15] Thorsen T, Holt T. The potential for power production from salinity gradients by pressure retarded osmosis. *J. Membr. Sci* 2009; 335: 103-110, <http://10.1016/j.memsci.2009.03.003>
- [16] Xu Y, Peng X, Tang CY, Fu QS, Nie S. Effect of draw solution concentration and operating conditions on forward osmosis and pressure retarded osmosis performance in a spiral wound module. *J. Membr. Sci* 2010; 348: 298-309, <http://10.1016/j.memsci.2009.11.013>
- [17] Achilli A, Childress AE. Pressure retarded osmosis: from the vision of Sidney Loeb to the first prototype installation - Review. *Desalination* 2010; 261: 205-211, <http://10.1016/j.desal.2010.06.017>
- [18] Ramon GZ, Feinberg BJ, Hoek EMV. Membrane-based production of salinity-gradient power. *Energy Environ. Sci* 2011; 4: 4423-4434, <http://10.1039/C1EE01913A>
- [19] Yip NY, Elimelech M. Performance limiting effects in power generation from salinity gradients by pressure retarded osmosis. *Environ. Sci. Technol* 2011; 45: 10273-10282, <http://10.1021/es203197e>
- [20] Yip NY, Elimelech M. Thermodynamic and energy efficiency analysis of power generation from natural salinity gradients by pressure retarded osmosis. *Environ. Sci. Technol* 2012; 46: 5230-5239, <http://10.1021/es300060m>
- [21] Yip BE, Elimelech M. Membrane-based processes for sustainable power generation using water. *Nature*, 2012; 488: 313-319, <http://10.1038/nature11477>
- [22] Kim YC, Elimelech M. Potential of osmotic power generation by pressure retarded osmosis using seawater as feed solution: analysis and experiments. *J. Membr. Sci* 2013; 429: 330-337, <http://10.1016/j.memsci.2012.11.039>
- [23] Wang X, Huang Z, Li L, Huang S, Yu SH, Scott K. Energy generation from osmotic pressure difference between the low and high salinity water by pressure retarded osmosis. *J. Technol. Innov. Renew. Energy* 2013; 1: 122-130
- [24] Alsvik I, Hägg MB. Pressure retarded osmosis and forward osmosis membranes: materials and methods. *Polymers* 2013; 5: 303-327, <http://10.3390/polym5010303>
- [25] Klaysom C, Cath TY, Depuydt T, Vankelecom IFJ. Forward and pressure retarded osmosis: potential solutions for global challenges in energy and water supply. *Chem. Soc. Rev* 2013; 42: 6959-6989, <http://10.1039/C3CS60051C>
- [26] Dinger F, Tröndle T, U. Platt. Optimization of the energy output of osmotic power plants. *J. Renew. Energy*, 2013; e496768, <http://10.1155/2013/496768>
- [27] He W, Wang Y, Shaheed MH. Energy and thermodynamic analysis of power generation using a natural salinity gradient based pressure retarded osmosis process. *Desalination* 2014; 350: 86-94, <http://10.1016/j.desal.2014.07.015>
- [28] Helfer F, Lemckert C, Anissimov YG. Osmotic power with pressure retarded osmosis: theory, performance and trends - a review. *J. Membr. Sci* 2014; 453: 337-358, <http://10.1016/j.memsci.2013.10.053>
- [29] Hong SS, Ryoo W, Chun MS, Lee SO, Chung GY. Numerical studies on the pressure-retarded osmosis (PRO) system with the spiral wound module for power generation. *Desalin. Water Treat* 2014; 52: 6333-6341, <http://10.1080/19443994.2013.821041>
- [30] Jia Z, Wang B, Song S, Fan Y. Blue energy: current technologies for sustainable power generation from water salinity gradient. *Renew. Sustain. Energy Rev* 2014; 31: 91-100, <http://10.1016/j.rser.2013.11.049>
- [31] Straub AP, Lin S, Elimelech M. Module-scale analysis of pressure retarded osmosis: performance limitations and implications for full-scale operation. *Environ. Sci. Technol* 2014; 48: 12435-12444, <http://10.1021/es503790k>
- [32] Buonomenna MG, Bae J. Membrane processes and renewable energies. *Renew. Sustain. Energy Rev* 2015; 43: 1343-1398, <http://10.1016/j.rser.2014.11.091>
- [33] Han G, Zhang S, Li X, Chung TS. Progress in pressure retarded osmosis (PRO) membranes for osmotic power generation. *Progress in Polymer Science* 2015; 51: 1-27, <http://10.1016/j.progpolymsci.2015.04.005>
- [34] McGinnis RL, McCutcheon JR, Elimelech M. A novel ammonia-carbon dioxide osmotic heat engine for power generation. *J. Membr. Sci* 2007; 305: 13-19, <https://doi.org/10.1016/j.memsci.2007.08.027>
- [35] Reimund KK, Kevin K., Jeffrey R. McCutcheon, and Aaron D. Wilson. Thermodynamic analysis of energy density in pressure retarded osmosis: the impact of solution volumes and costs. *Journal of Membrane Science* 2015; 487: 240-48, <https://doi.org/10.1016/j.memsci.2015.03.076>

- [36] Wilson, Aaron D. Design of the next-generation fo draw solution. in rational design of next-generation nanomaterials and nanodevices for water applications. international water association (IWA). 2016; 15: 103-130, <https://doi.org/10.2166/9781780406862>.
- [37] Miller JE, Evans LR. 2006-4634-Forward Osmosis: A new approach to water purification and desalination. Sandia report. Sandia National Laboratory, July 2006.
- [38] Kays, William; Crawford, Michael; Weigand, Bernhard. 2004. Convective heat and mass transfer, 4E. McGraw-Hill Professional
- [39] Incropera, F.P; DeWitt D.P. 1990. Fundamentals of heat and mass transfer (3rd ed.). John Wiley & Sons. p. 28.
- [40] Getling, A.V. 1998. Rayleigh-Bénard convection : structures and dynamics (Reprint. ed.). Singapor
- [41] Fedosov A. I. 1956. Thermocapillary motion. Zhurnal Fizicheskoi Khimii 30, N2, p. 366-373
- [42] Arias FJ. A first estimate for a pressure retarded osmosis-driven thermosyphon. Journal Solar Energy 2018; 159: 962-965. <https://doi.org/10.1016/j.solener.2017.10.064>
- [43] Arias FJ, De Las Heras SA. The brinesiphon: a homolog of the thermosiphon driven by induced salinity and downward heat transfer. Journal Solar Energy 2017; 153: 454-458. <https://doi.org/10.1016/j.solener.2017.05.091>
- [44] Handbook of Chemistry and Physics, 27th edition, Chemical Rubber Publishing Co., Cleveland, Ohio, 1943
- [45] Chacha M, Saghir MZ. Solutal-thermo-diffusion convection in a vibrating rectangular cavity. International Journal of Thermal Sciences 2005; 44: 1: 1-10. <https://doi.org/10.1016/j.ijthermalsci.2004.04.013>
- [46] Chacha M, Faruque D, Saghir MZ, Legros JC. Solutal thermodiffusion in binary mixture in the presence of g-jitter International Journal of Thermal Sciences 2002; 41: 10: 899-911. [https://doi.org/10.1016/S1290-0729\(02\)01382-0](https://doi.org/10.1016/S1290-0729(02)01382-0)
- [47] Srinivasan Seshasai, Dejmeck M, Saghir MZ. Thermo-solutal-diffusion in high pressure liquid mixtures in the presence of micro-vibrations. International Journal of Thermal Sciences 2010; 49: 9: 1613-1624. <https://doi.org/10.1016/j.ijthermalsci.2010.04.018>
- [48] Yip YN, Elimelech M. Thermodynamic and energy efficiency analysis of power generation from natural salinity gradients by pressure retarded osmosis. Environ. Sci. Technol 2012; 46: 5230-5239. <https://doi.org/10.1021/es300060m>
- [49] Lin S, Straub AP, Deshmukh A, Elimelech M. Thermodynamic limits of extractable energy by pressure-retarded osmosis. Journal Energy & Environmental Science 2014; 7: 2706-2714. <https://doi.org/10.1039/C4EE01020E>
- [50] Straub AP, Deshmukh A, Elimelech M. Pressure-retarded osmosis for power generation from salinity gradients: is it viable?. Journal Energy & Environmental Science 2016; 9: 31-48. <https://doi.org/10.1039/C5EE02985F>
- [51] Planck M. Treatise on thermodynamics. 1917 2nd edn. Longmans Green & Co, London.
- [52] Garcia AV, Thomsen K, Stenby EH. Prediction of Mineral Scale Formation in Geothermal and Oilfield Operations using the Extended UNIQUAC Model. Part I: Sulphate Scaling Minerals, (Geothermics, 34(2005)61-97) <https://doi.org/10.1016/j.geothermics.2004.11.002>
- [53] Garcia AV, Thomsen K, Stenby EH. Prediction of Mineral Scale Formation in Geothermal and Oilfield operations using the Extended UNIQUAC Model. Part II: Carbonate Scaling Minerals, (Geothermics 35(2006)239-284) <https://doi.org/10.1016/j.geothermics.2006.03.001>
- [54] Rodriguez JA, Ruiz JJ, Urieta JS. 2000. Termodinámica química. Síntesis. Volumen 5 de Ciencias Químicas. ISBN 84-7738-581-5.
- [55] Linert W. Highlights in Solute-Solvent Interactions. Springer Science & Business Media, 11 dic. 2001.
- [56] Mersmann A. Crystallization Technology Handbook. CRC Press, 8 may. 2001
- [57] Magalhaes MCF, Konigsberger E, May PM, Hefter G. Heat Capacities of Concentrated Aqueous Solutions of Sodium Sulfate, Sodium Carbonate, and Sodium Hydroxide at 25°C. J. Chem. Eng. Data 2002, 47, 590-598. <https://doi.org/10.1021/je010314h CCC>
- [58] Bhatnagar ON, Campbel AN. Experimental data from Bhatnagar and Campbell, Osmotic Coefficients of Sodium Sulphate in water from 50 to 150°C, Canadian journal of chemistry 59(1981)123-126. <https://doi.org/10.1139/v81-019>
- [59] Smoluchowski M. Mathematical theory of the kinetics of coagulation of colloidal solutions. Z, Phy, Chem 1917; 92: 219.
- [60] Harrison R.G., Todd P., Rudge S.R., Petrides P.D., Bioseparation science and engineering. New York, Oxford University Press. 2003.
- [61] Kevin J. Wilkinson, Jamie R. Lead. Environmental colloids and particles: behaviour, separation and characterisation. IUPAC series on Analytical and Chemistry of Environmental System. 2007.
- [62] Darby, Ron (2001). Chemical Engineering Fluid Mechanics (2nd ed). CRC Press. p. 64.
- [63] Camp a T.R., Stein P.C. 1943. Velocity gradients and internal work in fluid motion. Boston Soc. Civ. Eng. 30, p.219.
- [64] Mulder, M, Basic principles of membrane technology. Kluwer Academic Pub, U.S.A., 1996
- [65] Salvador De Las Heras. Mecánica de fluidos en ingeniería. Publicacion UPC. 2012
- [66] Wilson AD, Stewart FF. Deriving osmotic pressures of draw solutes used in osmotically driven membrane processes J. Membr. Sci 2013; 431: 205-211, 10.1016/j.memsci.2012.12.042
- [67] Lewis GN, Gilbert Newton. The osmotic pressure of concentrated solutions, and the laws of the perfect solution. Journal of the American Chemical Society. 1908; 30(5): 668-683. doi:10.1021/ja01947a002. ISSN 0002-7863
- [68] Salis A, Ninham BW. Models and mechanisms of Hofmeister effects in electrolyte solutions, and colloid and protein systems revisited. Chem Soc Review 2014; 43: 7358-7377